euspen's 26th International Conference & Exhibition, Krakow, PL, June 2026
www.euspen.eu

A new backlight imaging method for in-machine measurement of flank wear

Lukas Jansen[1], Knut Sørby[1]

[1]Department of Mechanical and Industrial Engineering, NTNU Norwegian University of Science and Technology, Trondheim, Norway
lukas.jansen@ntnu.no

Abstract
A new method for in-machine measurement of tool wear in milling machines, based on backlit imaging, is presented. An established approach for measuring flank wear with this type of equipment is to estimate the wear from tool diameter reduction. However, this approach is highly sensitive to small errors in the diameter measurement, making it necessary to measure the diameter within single digit micrometer values.
To address these limitations, we propose a new method for estimating flank wear, based on the assumption that flank wear land is a part of a cylindrical surface coaxial to the tool axis. In the proposed method, images of the tool are taken while incrementally rotating it. When measuring the diameter based on points on the worn area, the diameter value is constant across multiple images. The results show good agreement between the new proposed method and conventional microscope measurements.

Backlight imaging; Flank wear measurement; Optical sensor; Machining

1. Introduction

Tool wear is one of the major, uncertainties in machining making it one of the main limitations for cost minimization in automated machining processes. Hernandez et al.[1] found that the average tool is retired well before it is worn out, making use of only half of the possible lifetime. They also found that some tools are used beyond their useful life, threatening damage to the workpiece. Colantonio et al. [2] look at different imperfect tool replacement strategies. They conclude that cost savings of 8.1% and a reduction in CO_2 equivalent emissions of 8.7% can be achieved with tool monitoring as compared to replacing the tools after a fixed usage time. In their scenario, which includes tool, workpiece and machine, the tool is responsible for 70% of the CO_2 equivalent emissions for parts production, further highlighting the need to use tools to their full potential. This is enabled by monitoring the tool condition.

While measuring tool wear is an established process and described in ISO standard 8688-2 (for milling tools) [3], the method is not intended for in-process measurement of tools for condition monitoring.

Automating tool wear measurements within the machine is of great interest and has successfully been implemented by others in experimental environments. While many different solutions using direct and indirect measurements of tool wear and its effects have been presented, we focus on direct optical approaches. Most often images of the tool are taken, and the captured information is then used to measure the wear on the flank of the tool directly [4-8]. The automated processes that look at the flank of the tool directly face many difficulties in practice due to changing conditions such as illumination and tool coatings with different reflectiveness, making them less reliable.

An alternative approach is the use of backlighting which leads to only the tool silhouette being visible to the camera. This method is more robust because it is independent of the tool's visual appearance. Liang et al. [9] presented a method to use the reduction in the tool diameter and the flank clearance angle to calculate tool wear. A disadvantage of this approach is that the tools' flank clearance angle is typically not published by the tool manufacturer, making a measurement of it necessary. Additionally, the estimation of flank wear from tool diameter reduction gets more complex since the clearance surfaces of the tool rarely have simple geometries but instead are shaped by multiple radii. Lastly the tool diameter must be measured very precisely to get reliable flank wear measurements. One unit length in tool diameter reduction leads to a 5 to 10 units increase of flank wear for common clearance angles of 6 to 12 degrees.

To make use of the benefits of backlit optical tool wear measurements while omitting some of its disadvantages we suggest a new measurement method.

In the method section, the idea of the new measuring process is introduced and the experimental set up is presented. Next, the process as well as the reference measurements are presented and then discussed. Finally, the conclusion of the paper and an outlook on further work is given.

2. Method

Flank wear is the most widely used measurement of tool wear and tends to be the dominant wear type in machining of metals with conventional cutting parameters.

The effect of flank wear on the tool geometry is easily visualized in a turning tool, where it leads to a loss of the cutting edge. Due to the flank's clearance angle, a wear zone that increases in length with progressing wear is formed (*Figure 1*).

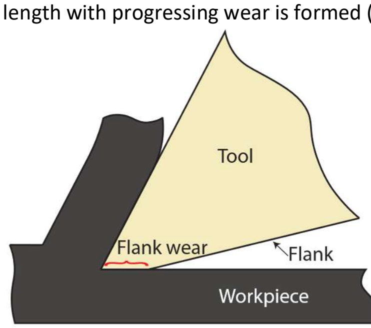

Figure 1. Flank wear in orthogonal cutting.

The increase of cutting force that correlates with flank wear is caused by the increased area on the tool that rubs against the work piece [10]. It is also possible to measure a decrease in electrical resistance between tool and workpiece [11]. This is caused by an increasingly larger contact zone between tool and workpiece.

Considering the increase in cutting force and decrease in resistance across the tool-workpiece interface we assume that the entire flank wear zone is in contact with the workpiece.

In milling, the tool wear is generated by a rotational movement of the tool. The presented measurement method uses the assumption that the worn area is a part of an imaginary cylinder that is coaxial with the tool axis. Figure *2* shows an illustration of the coaxial wear zone.

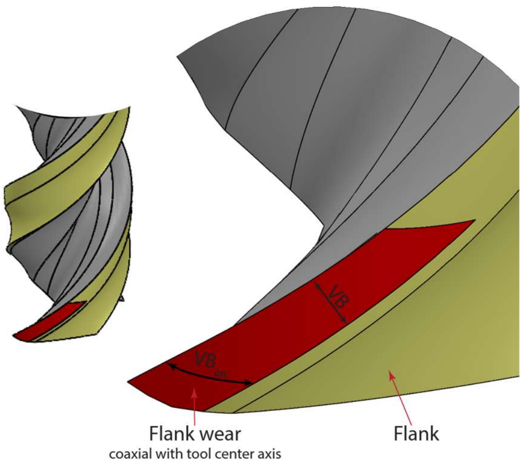

Figure 2. Flank wear on a milling tool (red coloured area). The flank wear land is assumed to be part of a cylindrical surface.

The outcome of the measurement process is the length of the flank wear zone measured from the current cutting-edge up to the end of the flank wear parallel to the cutting direction, called VB_{arc} here after.

To capture VB_{arc} a camera-based sensor (CU2 Tool) manufactured by Conoptica AS is used. The sensor is usually used as a tool setter and is therefore built such that it can permanently remain within the milling machine's work envelope.

A 10 mm end mill with a helix angle of 32 degrees manufactured by UOP is used to test the process. Controlled flank wear is artificially created with the tool in the spindle of the milling machine. A grinder is placed on the machine table and tilted slightly. With the spindle engaged, the tool is then brought into contact with the grinding wheel. This creates tapered flank wear on the tool. As a reference, the artificially created flank wear is measured with an Alicona G4 focus variation microscope.

3. Results

3.1. Measuring VB_{arc}

To measure VB_{arc}, images of one side of the tool are taken. Since backlighting is used, the silhouette of the tool is visible. The edge of the silhouette represents the outermost visible contour of the tool. When spinning the tool, each point on that contour appears to move in and out in the recorded images. By rotating a sharp tool and plotting the edge position, a parabola shaped diagram is created. This shape arises because the cutting edge is the part of the tool that lies farthest from its central axis. As it approaches an orthogonal orientation relative to the camera's line of sight, its apparent radial position increases before decreasing again.

Following our earlier assumption of the coaxiality of the flank wear region to the tool's central axis, plotting a similar diagram for a worn tool will lead to a different shape of the curve. Instead of a clear peak, the diagram will show a plateau, the length of which corresponds to VB_{arc}. A representation of the measurement principle and the resulting plots for a sharp and a worn tool can be seen in *Figure 3*.

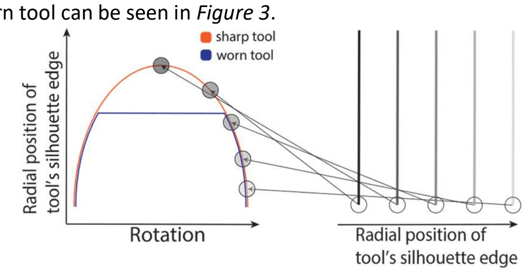

Figure 3. Tool silhouette edge radial position plot based on edge position across multiple images.

The distance the cutting-edge travels along an arc (T_{arc}) between two images depends on the rotational speed of the tool (n) as well as the frame rate at which the camera takes images (f_s).

Since both values can be adjusted within the equipment's limits it is practical to define T_{arc} so, that it is sufficiently small to capture the expected flank wear. This can be done for a maximum allowable flank wear value as defined in ISO 8688-2 or if flank wear is to be tracked over time, by defining a resolvable minimum flank wear value. Since flank wear follows an S-shaped curve, with a high wear rate early on, and since smaller values of VB_{arc} are harder to resolve, it is practical to define T_{arc} such that it can resolve the flank wear after the initial wear phase. After defining T_{arc} the tool rotation between images, θ, can be calculated based on T_{arc} and the tool's cutting diameter, D:

$$\theta = \frac{T_{arc}}{\pi \cdot D} \cdot 360 \tag{1}$$

Since an unpractically high frame rate would be required to capture all images within one revolution of the tool, only one image per revolution is captured. For this the required frame rate (f_s) of the camera can be calculated:

$$f_s = n \cdot \frac{360 - \theta}{360} \tag{2}$$

3.2 Image processing

The developed measuring process is implemented in Python. The steps taken to get from the captured images to VB_{arc} measurements are seen in **Error! Reference source not found.**. The process can be divided into two parts, one which repeats the same step for one image at a time, and a second step that repeats the same process for one axial position along the cutting edge of the tool. The second step is based on the data extracted in the first step.

The rough edge position for each image is found using Canny [12] edge detection. Small gaps between the detected edges are then closed with morphological edge closing. To get a smooth and continuous edge, a spline curve is fitted. Since the tool silhouette extends to the limits of the image, the spline fit is not sufficiently defined at the ends. To prevent erratic spline fits the ends of the spline are defined based on the slope of the spline further into the image. This is acceptable since the edge slope changes only slowly.

With knowledge of the approximate edge location fine edge detection is done. Based on the work of Venkatachalam et al. [13], who compare different sub-pixel edge detection methods, quadratic edge detection is chosen for its high accuracy and relative simplicity.

Lines orthogonal to the rough silhouette edge are used as a guide to obtain the intensity of a set of neighbouring pixels across the edge. To the pixel intensities a cubic function is fitted and differentiated. The cubic function is used to avoid the

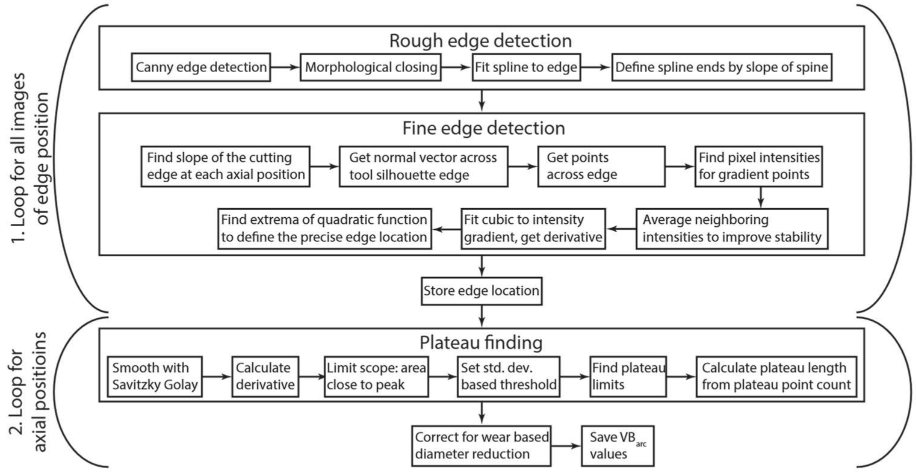

Figure 4. *Measuring process to determine VB_{arc} based on tool silhouette images.*

amplification of noise when directly differentiating the pixel intensities [14]. The quadratic function represents the change in intensity. The cutting-edge is located at the peak of the quadratic function where the intensity change is at its maximum. The process of finding an edge precisely based on a quadratic function is described by Seitz [15].

The fine edge location is determined in the same manner for every image and then stored. In the next step the edge position extracted over all images for one axial position is considered. The same steps are then repeated for all axial positions.

By plotting the edge points of one axial position, a diagram close to a parabola with a flat plateau on top is created (Figure 3). The number of data points that lie within that plateau determine VB_{arc}[1]. Therefore, the size of the plateau must be found. This is done based on the derivative of the data, which is equal to zero for a true plateau. Since the edge locations are collected from real images, there is some noise present in the data, which gets amplified in the derivative. To reduce that noise the edge position data is smoothed using a Savitzky Golay [14] filter. Since this does not fully eliminate noise, a threshold based on the standard deviation of the signal is set to define the data points to be part of the plateau. More noise in edge detection is seen in areas of the tool that are further from their peak radial position. This can be attributed to the measured point being further from the focus plane of the sensor resulting in a more blurred image. To avoid these high noise areas, the scope for defining the standard deviation-based threshold is limited to an area close to the absolute maximum of the cutting-edge position.

As seen in Equation 1, the length of the arc between images depends on the diameter of the tool, which decreases with wear. To compensate for this, we estimate the tool diameter reduction by comparing the maximum radial silhouette edge location in an unworn area to the local maximum radial silhouette edge location. Using the resolution of the optical sensor an approximate reduction of the tool diameter is calculated. It should be noted that this correction will contain some error itself due to the lenses distortion which we do not compensate for here.

Figure 5 shows the measured radial positions of the silhouette edge for all axial positions, as well as the found plateaus.

In *Figure 6*, VB_{arc} as calculated by the described process is plotted over the axial position.

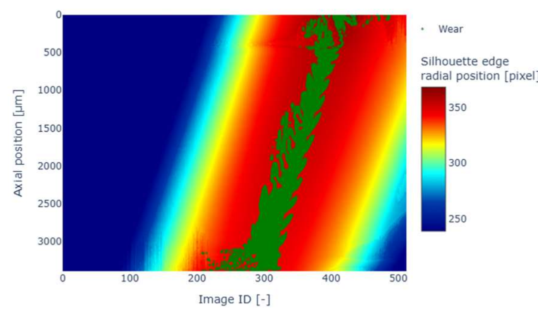

Figure 5. Radial position of silhouette edge development across images for all axial positions and found wear.

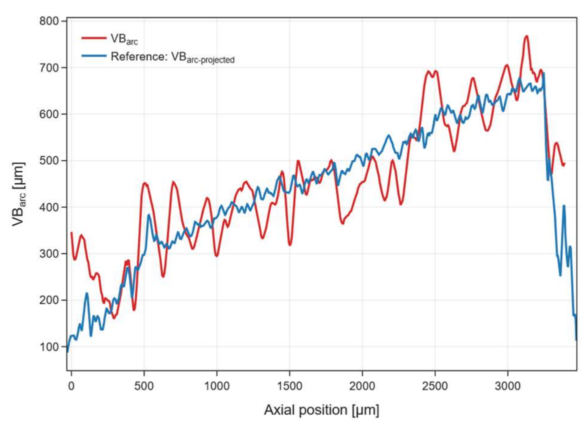

Figure 6. VB_{arc} as determined by the camera-based sensor and the focus variation microscopy-based reference measurement.

To evaluate the VB_{arc} measurements, they are compared to reference measurements taken with the focus variation microscope.

The base data exported from the microscope is a three-dimensional point cloud of the worn flute. This data is first cleaned of outliers and then separated into two dimensional slices along the tool's axis. It is also smoothed using a Savitzky

[1] Other approaches for determining the plateau size can be applied. Calculating the distance between the outermost points of the plateau yields less reliable results, as the plateau size is often overestimated due to outliers.

Golay filter. When plotting this data one slice at a time a diagram with a kink (breakpoint) at which the flank surface transitions into the worn zone is created. By finding and then plotting this point over all axial positions, the limits of the worn zone can be found (Figure 7).

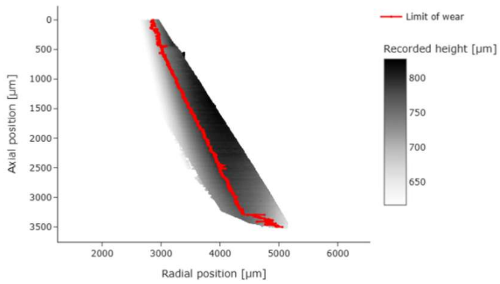

Figure 7. Wear area based on focus variation microscopy data.

For each y position, the distance between the cutting edge and the wear zones limit is calculated. The result is the projected length of VB_{arc}. Trials with fitting a circle section to the found sections of the wear zone, to get the non-projected length of VB_{arc} were prone to a large amount of noise that is larger than the small error from using the projected VB_{arc} length. The resulting plot of VB_{arc}-projected depending on the axial position can be seen in Figure 6.

4. Discussion of results

The resulting wear plots in Figure 6 show good agreement between the camera-based measurement and the reference measurement. This proves that measurement of wear on the flank of the tool is possible with the presented method, given that this wear is concentric to the tool axis. The camera-based results show more variation than the reference measurement, but small deviations in the mean value. This is likely caused by the difficulties in the detection of the plateau of the radial position curve. The camera-based measurement also detects wear in the unworn section (axial position < 450 µm). This is likely caused by the limitation of the plateau detection method when no actual plateau is present. The reference method does also have some limitation in detecting zero wear. This method is based on detection of a break point between the worn area and the unworn flank face.

Towards the bottom of the tool (axial position > 3200 µm) both measurements drop off steeply. This is due to the pointed tool geometry at the bottom, these measurements are not representative.

Considering the section between 450 µm and 3200 µm, the measurements have a relatively small bias of 2.97 µm, but a large average absolute deviation of 49 µm. This again is likely caused by deviations in the plateau or edge detection.

Looking at Figure 5 a repeating pattern can be seen, the cause of that pattern has not yet been determined.

5.Conclusion and outlook

A new method for measuring the length of the worn section along a tool's flank face is presented in this paper. It uses the assumption that the worn area is a cylindrical surface that is coaxial with the tool axis.

The main benefits of the method are its robustness to changes in the tool's optical properties due to use of backlit images and its independence of unavailable tool geometry data. It is also possible to deploy it within the machine tools work envelope. Measurements taken with the described process are compared to measurements from a focus variation microscope.

The measurements show good correlation in the development of wear for different levels of tool wear, showing that a detection of these coaxial flank wear zones is possible with the described process. Based on this, further work in the following areas needs to be undertaken: (1) The process variation is large and should be addressed by improving the algorithms used to find the cutting edge in the base images and the plateau size. (2) It is of interest to calculate VB as defined in ISO 8688-2, based on the proposed backlit method. For this some corrections like compensation of the helix angle and movement of the cutting edge under wear must be made.

References

[1] A. E. B. Hernández, T. Beno, J. Repo, and A. Wretland, 'Analysis of Tool Utilization from Material Removal Rate Perspective', *Procedia CIRP*, vol. **29**, pp. 109–113, 20153.

[2] L. Colantonio, G. Moroncini, O. Sénéchal, P. Dehombreux, F. Ducobu, and L. Equeter, 'Cost and Environmental Assessment of Tool Replacement Strategies Under Imperfect Wear Monitoring in Ti6Al4V Milling', *Int. J. Progn. Health Manag.*, vol. **16**, no. 4, Nov. 2025.

[3] *ISO 8688-2:1989-05 Tool life testing in milling; part 2: end milling*.

[4] S. Mehta, R. A. Singh, Y. Mohata, and M. B. Kiran, 'Measurement and Analysis of Tool Wear Using Vision System', in *2019 IEEE 6th International Conference on Industrial Engineering and Applications (ICIEA)*, Tokyo, Japan: IEEE, Apr. 2019, pp. 45–49.

[5] P. J. Bagga *et al.*, 'Experimental investigation of different NN approaches for tool wear prediction based on vision system in turning of AISI 1045 steel', *Int. J. Interact. Des. Manuf. IJIDeM*, vol. **17**, no. 5, pp. 2565–2582.

[6] C. Zhang and J. Zhang, 'On-line tool wear measurement for ball-end milling cutter based on machine vision', *Comput. Ind.*, vol. **64**, no. 6, pp. 708–719, Aug. 2013.

[7] A. Agarwal, N. Potthoff, A. M. Shah, L. Mears, and P. Wiederkehr, 'Analyzing the evolution of tool wear area in trochoidal milling of Inconel 718 using image processing methodology', *Manuf. Lett.*, vol. **33**, pp. 373–379, Sep. 2022.

[8] L. Fernández-Robles, G. Azzopardi, E. Alegre, and N. Petkov, 'Machine-vision-based identification of broken inserts in edge profile milling heads', *Robot. Comput.-Integr. Manuf.*, vol. **44**, pp. 276–283, Apr. 2017.

[9] R. Liang, Y. Li, L. He, and W. Chen, 'A novel image-based method for wear measurement of circumferential cutting edges of end mills', *Int. J. Adv. Manuf. Technol.*, vol. **120**, no. 11–12, pp. 7595–7608, Jun. 2022.

[10] J. Wang, C. Z. Huang, and W. G. Song, 'The effect of tool flank wear on the orthogonal cutting process and its practical implications', *J. Mater. Process. Technol.*, vol. **142**, no. 2, pp. 338–346, Nov. 200.

[11] M. Murata, S. Kurokawa, O. Ohnishi, M. Uneda, and T. Doi, 'Real-Time Evaluation of Tool Flank Wear by In-Process Contact Resistance Measurement in Face Milling', *J. Adv. Mech. Des. Syst. Manuf.*, vol. **6**, no. 6, pp. 958–970, 2012.

[12] J. Canny, 'A Computational Approach to Edge Detection', *IEEE Trans. Pattern Anal. Mach. Intell.*, **vol. PAMI-8**, no. 6, pp. 679–698, Nov. 1986.

[13] V. Venkatachalam and R. M. Wasserman, 'Comprehensive investigation of subpixel edge detection schemes in metrology', presented at the Electronic Imaging 2003, M. A. Hunt and J. R. Price, Eds, Santa Clara, CA, May 2003, p. 200.

[14] Abraham. Savitzky and M. J. E. Golay, 'Smoothing and Differentiation of Data by Simplified Least Squares Procedures.', *Anal. Chem.*, vol. **36**, no. 8, pp. 1627–1639, Jul. 1964.

[15] P. Seitz, 'Optical superresolution using solid -state cameras and digital signal processing', *Opt. Eng.*, vol. **27**, no. 7, Jul. 1988,